Materials Chemistry and Physics (2012). 137(2), 608-616.
DOI: http://dx.doi.org/10.1016/j.matchemphys.2012.10.010

Influence of vacuum hot-pressing temperature on the microstructure and mechanical properties of Ti—3Al—2.5V alloy obtained by blended elemental and master alloy addition powders

L. Bolzoni*, E.M. Ruiz-Navas, E. Gordo

Department of Materials Science, Universidad Carlos III de Madrid, Avda. de la Universidad 30, 28911 Leganés, Madrid, Spain
*Corresponding author. Tel.: +34 91 6249482; fax: +34 91 6249430. *E-mail address:* bolzoni.leandro@gmail.com (L. Bolzoni).

Abstract:
This study addresses the processing of near-net-shape, chemically homogeneous and fine-grained Ti—3Al—2.5V components using vacuum hot-pressing. Two Ti—3Al—2.5V starting powders were considered. On one side, hydride—dehydride (HDH) elemental titanium was blended with an HDH Ti—6Al—4V prealloyed powder. On the other side, an Al:V master alloy was added to the HDH elemental titanium powder. The powders were processed applying a uniaxial pressure of 30 MPa. The sintering temperatures studied varied between 900 °C and 1300 °C. The relative density of the samples increased with processing temperature and almost fully dense materials were obtained. The increase of the sin-tering temperature led also to a strong reaction between the titanium powders and the processing tools. This phenomenon occurred particularly with boron nitride (BN) coating, which was used to prevent the direct contact between titanium and graphite tools. The flexural properties of the Ti—3Al—2.5V samples increased with vacuum hot-pressing temperature and are comparable to those specified for wrought titanium medical devices. Therefore, the produced materials are promising candidates for load bearing applications as implant materials.

Highlights:

Almost fully dense Ti—3Al—2.5V alloy components are obtained by means of hot-pressing.
The bending properties of the Ti—3Al—2.5V alloy are studied in details.
The reaction that occurs between the Ti—3Al—2.5V powder and the BN coating is analysed.
Microstructural evolution of blending elemental and master alloy materials with the temperature.

Keywords:
Ti—3Al—2.5V, Prealloyed, Master alloy, Vacuum hot-pressing, BN—Ti interaction, Mechanical properties

1. Introduction

Titanium is characterised by the highest strength to density ratio (specific strength) among metals, outstanding corrosion resistance, excellent biocompatibility and resistance at high temperatures. This unique combination of properties makes it suitable for different applications in many industries. Nevertheless, the employment of titanium and its alloys has always been limited to high performing industries, particularly the aeronautical industry. This is because of both the high extraction and production costs of titanium in comparison to other structural metals such as aluminium or steel. The high extraction costs are mainly due to the great affinity that titanium has for interstitials elements such as oxygen, nitrogen and carbon. These elements are difficult to eliminate and, even if their percentage is relatively low, they significantly lower the ductility and fatigue properties of titanium [1,2]. The high production costs are a result of the poor machinability as a consequence of the low thermal conductivity of titanium.

Titanium alloys are, generally, preferred to other metallic biomaterials, such as precious metals, due to its superior biocompatibility and corrosion resistance in conjunction with its low density and elastic modulus similar to that of human bones [3]. The Ti—3Al—2.5V titanium alloy was developed for aircraft hydraulic and fuel systems but is currently also used to fabricate medical and dental implants as well as sports equipments. This alloy is referred to as “half 6—4” because it is intermediate in strength in comparison with unalloyed titanium and Ti—6Al—4V alloy. It is classified as a near-alpha alpha-beta alloy or super-alpha titanium alloy [4].

Among the different fabrication processes, powder metallurgy (PM) techniques offer significant advantages in terms of material yield and number of production steps [5]. This is because most PM techniques are near-net-shape or net-shape processes. Generally, the powder metallurgy of titanium is split into two main approaches as functions of their powder production method: pre-alloyed (PA) and blending elemental (BE) powders. PA powders used to be more expensive and were characterised by spherical morphology because they were produced using atomisation techniques. For this reason, PA powders were normally processed with advanced techniques such as hot isostatic pressing (HIP) or metal injection moulding (MIM). On the other hand, the BE powders were produced by mixing an elemental titanium sponge powder with elemental alloying powders or with master alloys (MA). BE powders were normally characterised by an irregular morphology and, consequently, they were suitable for the conventional powder metallurgy route of pressing and sintering (P&S).

The problem with the employment of titanium sponge powders obtained directly from the Kroll process is the presence of residual chlorides. These chlorides generate porosity filled with gas which is difficult to close during the sintering step and make the material practically unweldable. Currently, irregular shaped elemental titanium and PA titanium alloy powders can be obtained by the hydride–dehydride (HDH) process, which takes advantage of the great affinity of titanium for hydrogen to embrittle it, reducing it to powder by means of a comminution process. The employment of HDH powders eliminates the problems connected with the presence of the chlorides.

HDH powders can be processed by P&S to obtain products with properties similar to wrought materials but, typically, they suffer from residual porosity [6]. To enhance the densification of the powder, uniaxial pressure can be applied during the sintering step and, thus, the process is known as uniaxial hot-pressing. If the process is carried out under vacuum, such as in the case of titanium and its alloy, the prefix vacuum is added. Processing studies of vacuum hot-pressing of elemental titanium sponge powders [7,8] and HDH Ti–6Al–4V powders [9,10] are available in the literature but no works were performed for the Ti–3Al–2.5V alloy.

The aim of this work is to study the processing of near-net-shape, chemically homogeneous and fine-grained Ti–3Al–2.5V components using vacuum hot-pressing. In particular, the influence of processing temperature on the microstructure and on the final properties was studied. The flexural properties of the produced materials were measured due to the possible employment of the studied alloy for the production of load bearing biomedical devices. The percentages of interstitial elements were determined and the interaction between the titanium powders and the processing tools analysed in detail because these parameters significantly influence mechanical behaviour.

2. Experimental procedure

The starting materials for this study were: an HDH prealloyed Ti–6Al–4V powder (Se-Jong Materials), an HDH elemental titanium powder and an Al:V master alloy (both supplied by GfE Gesellschaft für Elektrometallurgie mbH). The Ti–3Al–2.5V powders used to study the influence of vacuum hot-pressing temperature on the final properties and microstructure were obtained by means of the blending elemental approach. The HDH elemental titanium powder was blended with the HDH prealloyed Ti–6Al–4V powder and the produced powder was designated Ti32-BE. The same HDH elemental titanium powder was mixed with the Al:V master alloy and labelled Ti32-MA. The description of the production method and of the parameters employed to fabricate these powders can be found elsewhere [11].

Ti32-BE and Ti32-MA were fabricated by mixing appropriate ratios of the starting powders in a turbula mixer. The prepared powders were characterised in terms of their particle size distribution and chemical makeup (content of interstitials: oxygen, nitrogen and carbon). The particle size distribution and the maximum size of the powders (D_{max}) were obtained with a laser beam Mastersizer 2000 particle size analyser. Oxygen and nitrogen contents were measured with the inert gas fusion method using a LECO TC500 analyser. Carbon content was determined by the combustion technique using a LECO CS200 analyser. Chemical analyses were performed using several different ASTM standards: ASTM E1409 for oxygen, ASTM E1937 for nitrogen and ASTM E1941 for carbon.

The preparation of the mould for the vacuum hot-pressing experiments is illustrated in Fig. 1 and it can be summarised as follows:

- insert the lower graphite punch into the mould;
- line the inner of the graphite mould with a low reactivity graphite foil;
- place a graphite disc with the top face coated with a high temperature ceramic boron nitride (BN) spray to prevent the reaction between titanium and the graphite tools and facilitate mould release;
- pour and level the loose powder;
- place a graphite disc with the bottom face coated with the BN spray;
- cold uniaxially press the whole assembly at approximately 18 MPa.

During the study, three sintering temperatures, namely 900 °C, 1100 °C and 1300 °C, were used. The dwell time at maximum temperature was set to 1 h for 900 °C and 1100 °C and 30 min for 1300 °C. It is worth mentioning that the time selected for each

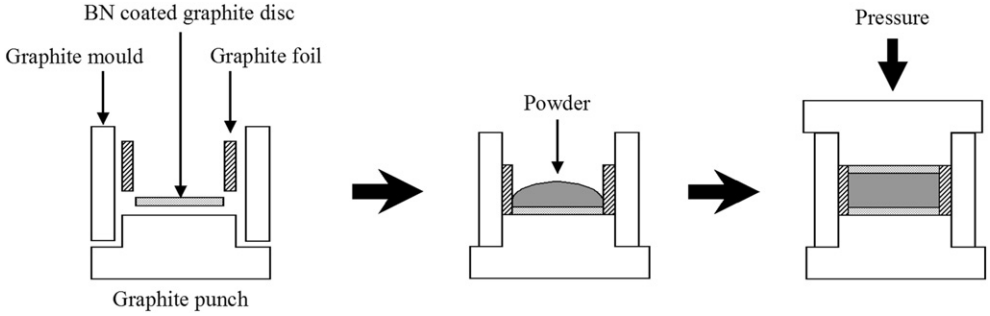

Fig. 1. Sketch of the hot-pressing process.

sintering temperature was dictated by the need to assure an effective dwell time of 30 min due to the delay induced by the inertia of the heating system. This delay can be clearly seen in Fig. 2, which shows the graph of the vacuum hot-pressing cycle used to sinter the powders at 900 °C. The control of the temperature was performed by means of thermocouples placed directly in contact with the graphite mould, which guaranteed precision of ±5 °C. Fig. 2 shows also that during vacuum hot-pressing experiments the temperature and applied pressure were increased simultaneously. Consequently, the maximum temperature and the maximum uniaxial pressure of 30 MPa were reached at the same time. The heating rate employed was 10 °C min^{-1} and a minimum vacuum level of 10^{-1} mbar was guaranteed. Cooling of the samples was performed by switching off the heating elements (furnace cooling) with simultaneous relief of the applied pressure. From Fig. 2, it can also be seen that the densification rate (measured by the displacement of the punch) went to zero approximately 10 min after the powder reached maximum temperature.

Once obtained, the hot-pressed specimens were taken from the graphite mould and their surfaces were sandblasted to clean them. The density of the samples was determined by Archimedes' method and the relative density values were calculated using the nominal values of the density of the wrought alloy (4.48 g cm^{-3}) [4].

Preparation of the specimens for microstructural analysis was done using the following metallographic route: grinding with SiC paper (320), polishing with 9 μm diamond suspension and final fine polishing with silica solution. The microconstituents were revealed by means of etching with Kroll's reagent (3 ml HF + 6 ml HNO_3 + 100 ml H_2O). The microstructures were analysed using an Olympus GX71 optical microscope.

Interstitials contents (oxygen, nitrogen and carbon) were measured using the LECO analysers described previously for the characterisation of the starting powders.

The surfaces of the samples were analysed using a Philips XL-30 SEM (backscatter mode) to study the nature of the interaction between the titanium powders and the BN coating used to prevent direct contact of the powder with the graphite tools.

X-ray diffraction (XRD) patterns of the surfaces of the specimens were obtained using a Bruker AXS D8-Advance diffractometer equipped with a Cu Kα1 radiation source. Step scans for phase identification were carried out from $2\theta = 20–120°$ using a step size of 0.02° and a dwell time of 2 s at each position.

Concerning the mechanical properties, the variation in the hardness with sintering temperature was measured by means of a Wilson Wolpert Universal Hardness DIGI-TESTOR 930 tester performing HV30 measurements. The flexural properties (maximum bending strength and flexural strain) of the vacuum hot-pressed Ti–3Al–2.5V samples were measured using a Micro-Test three-point bending test machine using the ASTM B528 standard. Because the samples show pronounced plastic deformation before fracture, the yield strength of the vacuum hot-pressed was also measured. The yield strength values were obtained by means of the offset method. It is worth mentioning that the flexural properties were determined on two types of sample: as-sintered and ground. For ground specimens, the surfaces were removed because they were in contact with the BN coating during consolidation. The removal of the surfaces permitted to study the influence of the outer layer on the final mechanical properties.

3. Results and discussion

3.1. Characterisation of the prepared powders

Some basic physical and chemical features of Ti32-BE and Ti32-MA are reported in Table 1 where it can be seen that both powders are characterised by an irregular morphology. Concerning the data shown in Table 1, Ti32-MA has slightly larger particle size with respect to Ti32-BE, D_{max} values are 90 μm and 75 μm, respectively. The difference in particle size will, most likely, affect the mechanical properties since a larger particle usually results in larger microstructural features. On the other hand, smaller particle size corresponds with a higher specific surface area and, therefore, a greater amount of oxygen adsorbed onto the surface of the powder particles.

From Table 1, it can be seen that, actually, the Ti32-BE powder has a higher oxygen content that is in agreement with its smaller particle size while the Ti32-MA powder has a greater carbon percentage. It is worth mentioning that the Ti32-MA carbon value shown in Table 1 is not the effective amount of carbon dissolved in the powder but is due to the production process. This is because a wax was used as process control agent during the adjustment of the particle size of the Al:V master alloy by high energy ball milling. This wax is normally eliminated during the sintering of the powder [11].

3.2. Density of hot-pressed materials

The variation of the relative density of the vacuum hot-pressed samples with the processing temperature is shown in Fig. 3.

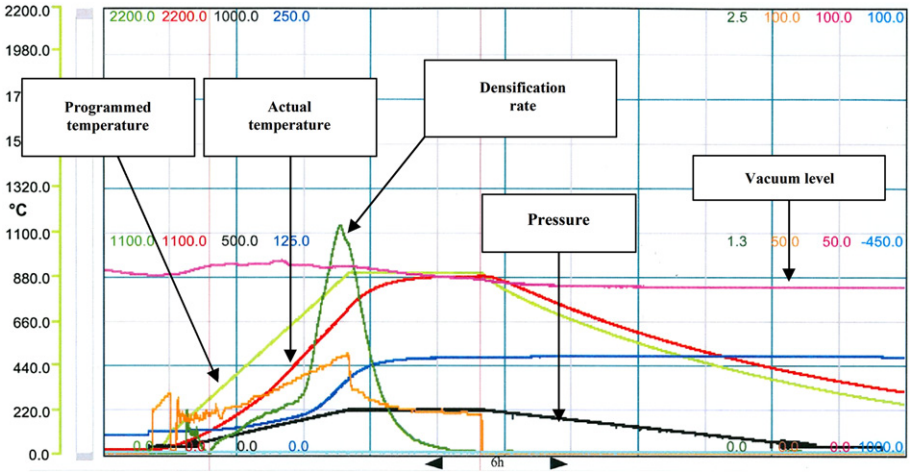

Fig. 2. Graph of the vacuum hot-pressing cycle used to sinter the powders at 900 °C.

Table 1
Particle size and chemical analysis of Ti32-BE (blended elemental) and Ti32-MA (master alloy addition) powders.

Material		Ti32-BE	Ti32-MA
Morphology		Irregular	Irregular
D_{max} [μm]		75	90
Chemical analysis [wt.%]	O	0.402	0.337
	N	0.0101	0.0118
	C	0.0120	0.0666

From Fig. 3, it can be seen that the relative density slightly increases with hot-pressing temperature and that the values reached for the two materials are similar (vary between 97.5% and 98.2%). Therefore, it can be stated that there is no clear influence from the properties of the powders and their production method, that is, the way the alloying elements are added to elemental titanium in order to obtain the desired final composition.

The relative density values shown in Fig. 3 are higher in comparison to the values normally obtained using the P&S process, which are approximately 95% of the theoretical density [12]. Furthermore, the data of Fig. 3 are comparable to those obtained by other authors when processing Ti–6Al–4V powders [9,13].

3.3. Microstructure of hot-pressed materials

Fig. 4 shows the microstructural evolution with hot-pressing temperature for Ti32-BE and Ti32-MA sintered at 900 °C, 1100 °C and 1300 °C. The optical micrographs were taken at the same magnification for comparison.

The microstructure of Ti32-BE and Ti32-MA hot-pressed at 900 °C (Fig. 4a and b) is characterised by porosity and undissolved particles (titanium and master alloy). For this case, the microstructure is not fully developed and it is composed of alpha phase. Because the processing temperature is below the nominal beta transus for the Ti–3Al–2.5V alloy, which is 935 °C [4], the typical laminar microstructure composed of α grain and α + β lamellae is not obtained.

The materials processed at 1100 °C (Fig. 4c and d) are characterised by a denser and more heterogeneous microstructure with no original undissolved particles. The microconstituents are α grains and α + β lamellae, where these lamellae are finer for Ti32-MA but more concentrated within restricted areas. These small and concentrated areas are most likely located near former master alloy particles and, therefore, near zones where locally the percentage of vanadium (β stabiliser) is higher. This result indicates that more thermal energy is invested in diffusing the alloying elements in the Ti32-MA powder in comparison with the Ti32-BE. Consequently, less energy is available for the development of the typical microstructure at this temperature. Nevertheless, the distribution of the alloying elements is not completely homogeneous for both the Ti32-BE and Ti32-MA as corroborated by means of EDS analysis.

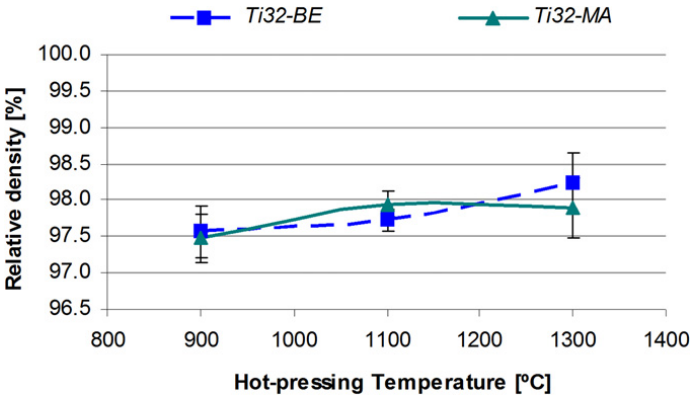

Fig. 3. Relative density as a function of hot-press temperature.

The main significant difference between the microstructure of the specimens hot-pressed at 1100 °C and 1300 °C (Fig. 4e and f) is the homogenisation of the alloying elements throughout the microstructure and the grain growth induced by the higher processing temperature. Thus, the samples vacuum hot-pressed at 1300 °C are characterised by the typical laminar microstructure of a slow cooled wrought Ti–3Al–2.5V alloy.

The comparison of the microstructural evolution of Ti32-BE and Ti32-MA indicates that there are not significant differences that can be highlighted. As a result, in the case of vacuum hot-pressing, there is no clearly better way of adding alloying elements to the elemental titanium powder to obtain the desired final composition.

3.4. Chemical analysis of hot-pressed materials

Regarding the results of the chemical analyses, for oxygen and carbon contents, a single value is reported in Fig. 5 for each processing temperature because no important differences were detected between the as-sintered and ground specimens. However, two trends are presented for nitrogen content in Fig. 6, one for the as-sintered and another for ground samples because significant differences were observed.

Analysing the oxygen content values shown in Fig. 5, it can be noticed that there is no oxygen pick-up with respect to the initial content of the powder (Table 1). The only exception is the value of the samples made out of the Ti32-MA powder processed at 1300 °C. Therefore, oxygen content of Ti32-BE stays constant at approximately 0.4 wt.% whereas oxygen content of Ti32-MA slightly increases from 0.34 wt.% to 0.39 wt.%. This result indicates that the level of vacuum used to process the material is appropriate to consolidate the Ti–3Al–2.5V powders. Moreover, no significant differences could be noticed in the behaviour of the two powders even though they have slightly different particle sizes. It was expected a greater increase of oxygen for Ti32-BE because of the higher specific surface area of the powder particles and, consequently, the higher the amount of oxygen adsorbed onto their surfaces.

For the case of carbon (Fig. 5), its percentage increases to a maximum value of 0.05 wt.% independent of temperature. The carbon pick-up is most likely due to the interaction with the graphite mould or the carbon rich atmosphere inside the hot-pressing chamber generated by the graphite tools at high temperature [14]. From the data in Fig. 5, it can also be seen that there is no well defined trend for the carbon content with processing temperature. Nevertheless, the maximum carbon content is, generally, lower than 0.08 wt.%, which is the limit specified for the wrought Ti–3Al–2.5V alloy [4]. It is worth mentioning that the lower carbon percentage found in the Ti32-MA samples in comparison with the content in the starting powder is due to the fabrication route of this alloy where some wax was added during milling of the master alloy as explained in the experimental procedure.

From Fig. 6, nitrogen percentage of the hot-pressed materials increases with the processing temperature. The increase is much more pronounced between 1100 °C and 1300 °C for both as-sintered and ground specimens. Furthermore, it can also be noticed that the difference in nitrogen content between the as-sintered and ground samples becomes more important with the increase in processing temperature. This result indicates that there is an interaction between the titanium powders and the BN coating applied to the graphite discs to prevent the direct contact of

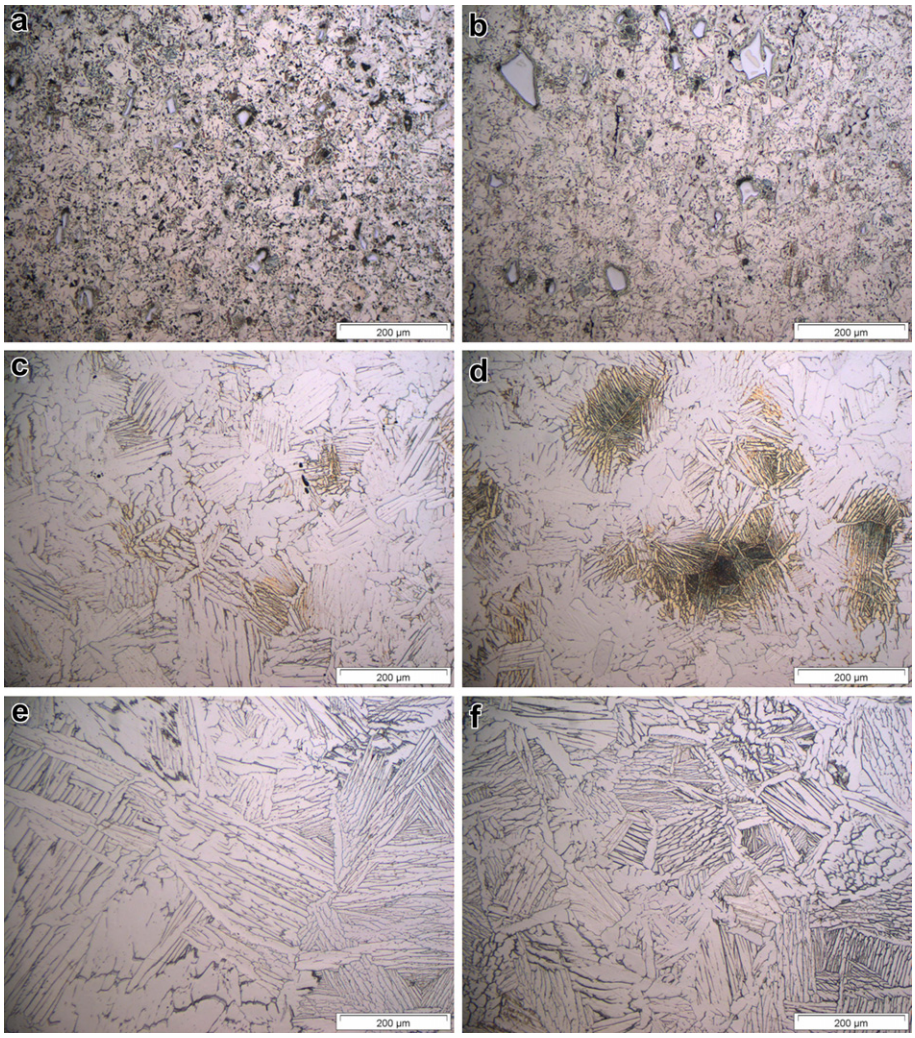

Fig. 4. Microstructure of Ti32-BE samples vacuum hot-pressed at: a) 900 °C, c) 1100 °C and e) 1300 °C; and Ti32-MA samples vacuum hot-pressed at: b) 900 °C, d) 1100 °C and f) 1300 °C.

titanium with the graphite tools. From the trends of nitrogen content, it can be stated that this interaction is strongly concentrated in the surface of the specimens even if there is some diffusion of nitrogen towards the alloy. It is worth mentioning that, in most of the cases the 0.03 wt.% nitrogen content limit specified for wrought Ti–3Al–2.5V alloy is fulfilled. The only exceptions are the values of the samples hot-pressed at 1300 °C which vary from 0.04 wt.% to 0.09 wt.%.

3.5. SEM analysis of the surfaces of hot-pressed materials

SEM analysis was carried out in order to identify and quantify the magnitude of the interaction between the powders and the BN coating. No significant differences were found between the behaviour of Ti32-BE and Ti32-MA. Thus, representative micrographs of the surfaces of the vacuum hot-pressed samples are shown in Fig. 7.

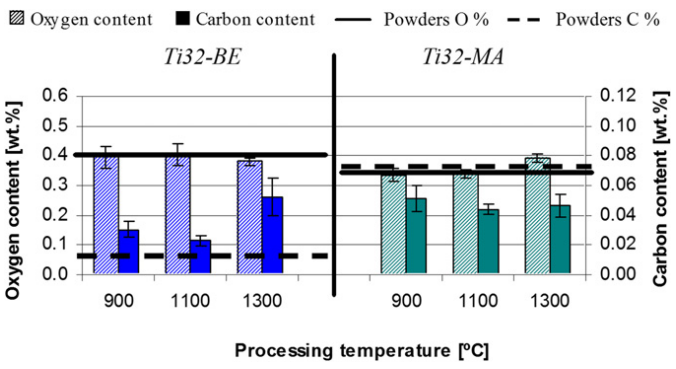

Fig. 5. Oxygen and carbon contents as a function of hot-press temperature.

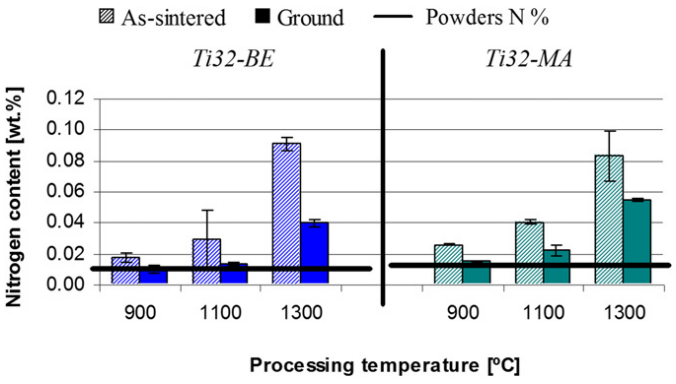

Fig. 6. Nitrogen content as a function of hot-press temperature.

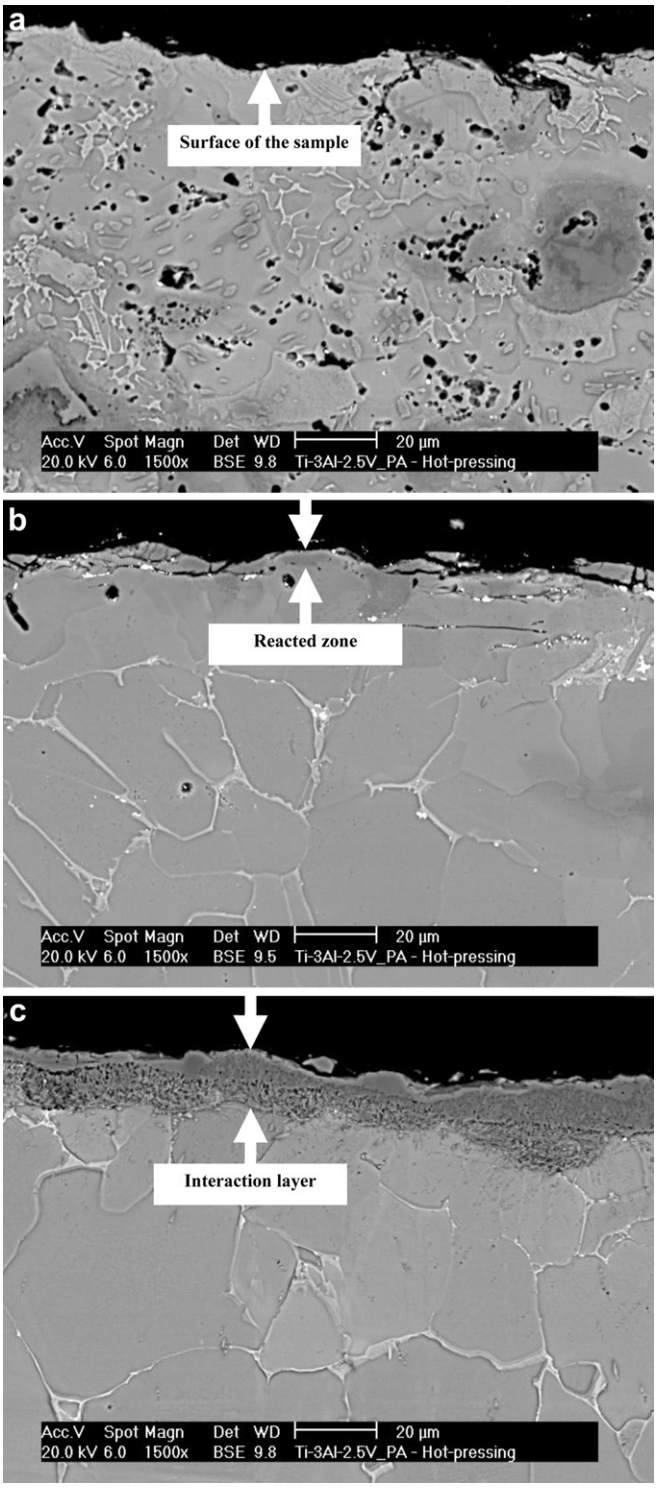

Fig. 7. SEM images (BE mode) of the surfaces of the vacuum hot-pressed specimens: a) 900 °C, b) 1100 °C and c) 1300 °C.

As can be seen in Fig. 7, it seems that there is no interaction between the powder and the BN coating when using a hot-pressing temperature of 900 °C. Nonetheless, based on the results of the nitrogen content (Fig. 6), it can be stated that some nitrogen from the BN coating diffuses towards the titanium matrix.

When the processing temperature is set to 1100 °C, the formation of an interaction layer of approximately 5–10 μm in thickness is observed, even if this layer is not actually uniform along the surface of the specimens.

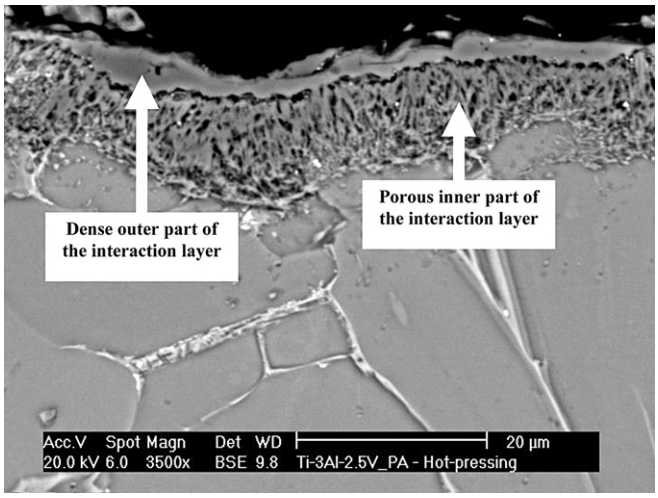

Fig. 8. Detail of the surfaces of samples vacuum hot-pressed at 1300 °C.

When hot-pressed at 1300 °C, the Ti–3Al–2.5V powders strongly react with the BN coating forming a uniform layer, which varies between 15 μm and 25 μm in thickness. This interaction layer is denser in the outer part and more porous in the inner part. The nature of the interaction layer is clearly visible in Fig. 8, which shows a magnified view of the surfaces of the specimens hot-pressed at 1300 °C.

EDS analysis was performed and it was determined that the reacted layer is composed of titanium and nitrogen but boron could not be detected due to the intrinsic detection limits of the equipment. Nitrogen mean content determined by EDS was approximately 5.4 wt.%, equivalent to 16.1 at.%.

3.6. XRD analysis of the surfaces of hot-pressed materials

To better understand the nature of the interaction between Ti32-BE and Ti32-MA powders with the BN coating, XRD analysis of the surfaces of the as-sintered samples was carried out. Only titanium compounds were detected on the surfaces of both materials. This fact is due to the greater affinity that titanium has for interstitial elements in comparison to those of aluminium and vanadium. The results of the XRD characterisation are presented in Fig. 9.

As can be seen in Fig. 9, the peaks detected and identified from the XRD pattern of the materials which were hot-pressed at 900 °C mainly refer to elemental titanium. Nonetheless, the position of these peaks is slightly shifted towards lower diffraction angles compared with the diffraction angles for elemental titanium. This is because the increased content of interstitial elements, such as nitrogen, in titanium induces an increase in both the "*a*" and "*c*" parameters of the unit cell [15,16]. Thus, it can be stated that due to the diffusion of nitrogen from the BN coating towards titanium, an interstitial solid solution of nitrogen in alpha titanium (α-Ti(N)) is formed.

Moreover, on the XRD pattern of the powder sintered at 900 °C, a peak corresponding to the Al:V master alloy used to produce the Ti32-MA powder was also detected (Al_2V_3). This finding confirms that this processing temperature is not high enough to promote complete diffusion of the alloying elements and homogenisation of the microstructure also indicated by in microstructural analysis.

The absence of boron or titanium boride in the XRD pattern of the specimens processed at 900 °C is mainly due to the higher

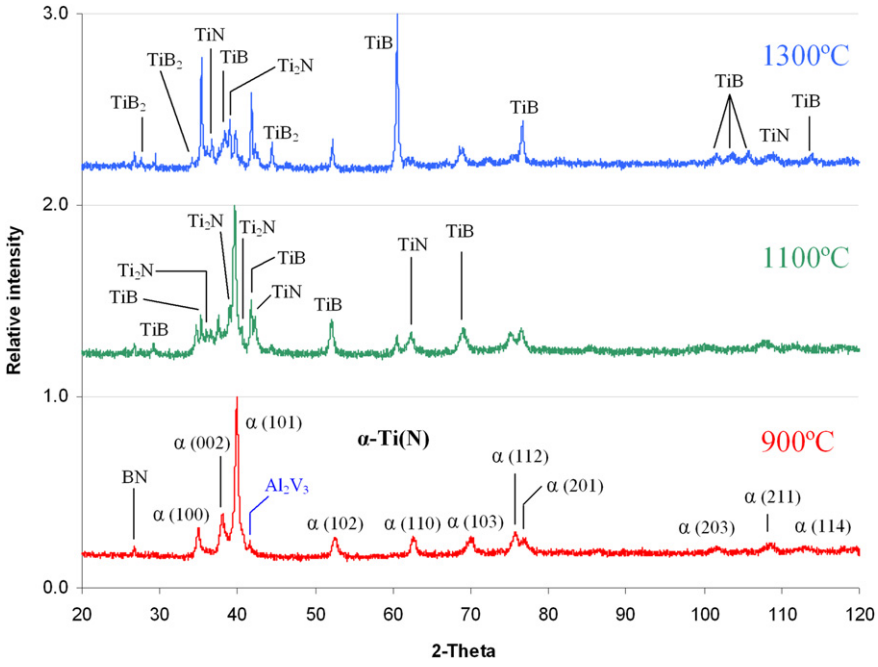

Fig. 9. XRD patterns ($2\theta = 20–120°$) of the surfaces of vacuum hot-pressed samples.

solubility of nitrogen in titanium with respect to boron. Actually, nitrogen solubility in beta titanium is 22 at.% whilst boron solubility in beta titanium is approximately 0.2 at.% [17]. Other experimental results discussed by Tomashik [18] in a review of the B–N–Ti ternary system indicate that TiN_{1-x} is a good diffusion barrier for boron at a temperature up to 1000 °C, which further helps to explain why boron was not detected in the specimens hot-pressed at 900 °C.

An increase in the hot-pressing temperature to 1100 °C leads to a higher degree of nitrogen diffusing into the titanium matrix (Fig. 6). This increase is high enough to promote the formation of compounds such as Ti_2N and TiN. Nonetheless, some peaks of the nitrogen rich solid solution α-Ti(N) are still present in the XRD pattern of the samples vacuum hot-pressed at 1100 °C. At this processing temperature boron, which was not detected at 900 °C, also diffuses towards the titanium powder forming stable compounds (TiB and TiB_2). According to thermodynamic calculations, the formation of titanium borides occurs with reactions that normally take place between titanium and boron nitride such as $Ti + 2BN \rightarrow TiB_2 + N_2$ and $Ti + BN \rightarrow TiB + 1/2N_2$ [19].

As seen during the SEM study of the surfaces of the specimens (Fig. 7), the interaction between titanium and the BN coating becomes stronger with the increase in processing temperature. This permits nitrogen to diffuse deeper towards the titanium matrix and allows boron to react strongly with titanium resulting in the XRD pattern of the materials processed at 1300 °C shown in Fig. 9. Consequently, the relative intensity of the peaks of the titanium nitrides decreases and that of titanium borides increases with respect to those found in samples processed at 1100 °C. These results are in agreement with the binary phase diagrams [17] and ternary system [18] where, according to thermodynamics calculation of chemical equilibrium for the BN–Ti system and studies about the reactions occurring at the BN–Ti interface [20], diffusion of BN towards titanium leads to the formation of new phases: namely, TiB_2 (directly at the interface) and TiN (further from the interface towards the material).

From the pattern of the specimens hot-pressed at 1300 °C it can be seen that TiB has a preferred growth direction [010], corresponding to the (020) plane, due to the strongest relative density of the peak at 60.6°. Based on the work performed by Faran et al., it can be stated that the dense outside part of the reacted layer (Fig. 8), is mainly composed of titanium borides whereas the porous interior part is made up of needle-like and preferentially oriented TiB grains and titanium nitrides [21].

Finally, independent of the processing temperature employed, the XRD patterns of the vacuum hot-pressed samples shows some BN, which was most likely not removed when cleaning the surface of the specimens by sandblasting.

3.7. Hardness of hot-pressed materials

The results of hardness measurements carried out on the cross-section of the specimens are displayed in Fig. 10. It is worth mentioning that because the measurements were taken in the cross-section of the samples, the values obtained are not influenced by the presence of the reacted layer formed in the surface of the specimens.

As can be seen in Fig. 10, the hardness of the hot-pressed Ti32-BE and Ti32-MA specimens increases with processing temperature with the exception of Ti32-BE processed at 1300 °C where the Vickers hardness is somewhat lower but has a greater standard deviation.

In more detail, the hardness of the samples hot-pressed at 900 °C is affected by the non-homogeneous distribution of the alloying elements throughout the titanium matrix. The Ti32-BE tends to be harder than the Ti32-MA because of the presence of the original PA Ti–6Al–4V particles and the higher oxygen content (Fig. 5). These factors justify also the higher hardness of Ti32-BE samples sintered at 1100 °C in comparison to Ti32-MA. Knowing that the microstructure of the specimens processed at 1300 °C is homogeneous (Fig. 4), the two materials reach similar hardness values because oxygen and nitrogen contents are slightly higher for the Ti32-MA but its relative density is somewhat lower (Fig. 3).

Finally, the amount of interstitials measured in the samples is responsible for the higher hardness of the vacuum hot-pressed Ti–3Al–2.5V samples in comparison with wrought Ti–3Al–2.5V alloy, whose nominal value is 267 HV [4]. Nevertheless, similar hardness

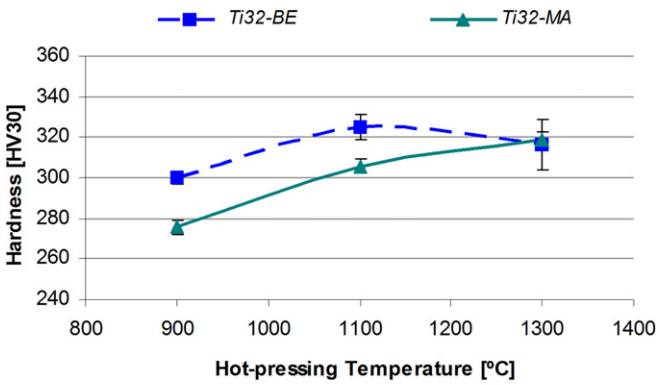

Fig. 10. Vickers hardness (HV30) as a function of hot-press temperature.

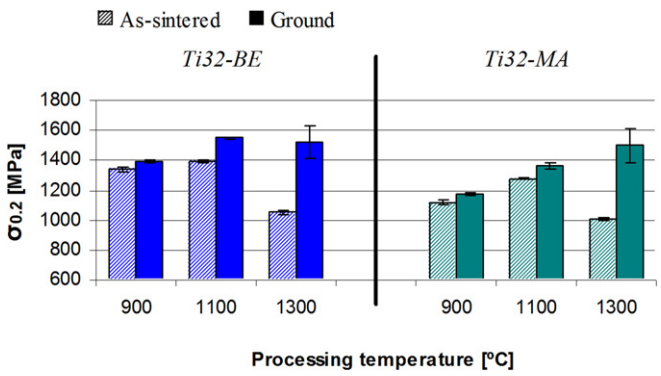

Fig. 12. Yield strength as a function of hot-press temperature.

values were obtained by processing these same materials by means of inductive hot-pressing [22].

3.8. Flexural properties of hot-pressed materials

Representative examples of load–deflection curves for each of the material studied are presented in Fig. 11. The curves refer to the specimens hot-pressed at 1100 °C and a comparison between the as-sintered and ground samples.

Analysing the representative behaviour of the load–deflection curves shown in Fig. 11, it can be seen that the flexural modulus of the two materials is similar. This result is mainly due to the comparable relative density values obtained when processing the two alloys by means of uniaxial hot-pressing techniques (Fig. 3). It can also be seen that the materials processed at 1100 °C do not behave as brittle materials and the samples fail after an appreciable amount of plastic deformation.

Remembering that the equation specified in the ASTM B528 standard for the calculation of the transverse rupture strength is applicable only to relatively brittle materials, $\sigma_{0.2}$ values were calculated. The comparison of the variation of these values versus processing temperature divided as a function of the grinding step is represented for each material in Fig. 12.

Analysing the yield strength mean values shown in Fig. 12 it can be seen that, for as-sintered samples the increase in processing temperature from 900 °C to 1100 °C leads to an increase in strength but further increases provoke a significant drop in this property. This behaviour could be explained by the fact that the strength of the specimens hot-pressed at 1100 °C is favoured by the decrease of residual porosity and by the homogenisation of the distribution of the alloying elements throughout the microstructure (see Fig. 4). At 1300 °C the strength of the as-sintered materials is mainly lowered by the presence of a thick reaction layer which embrittles the material.

The removal of the reacted surface by grinding becomes more important with the raising of the temperature for both materials. As can be seen in Fig. 12, at 900 °C, the difference in yield strength between the as-sintered and ground specimens of the same material is lower than 50 MPa. This difference becomes approximately 500 MPa when the powders are sintered at 1300 °C. Moreover, from Fig. 12, it can also be seen the removal of the interaction layer switches the behaviour of the materials because the yield strength always increases with the increase in hot-pressing temperature. The only exception is the strength value of Ti32-BE, where the strength of samples sintered at 1300 °C is similar to that of those processed at 1100 °C.

The strength of the samples hot-pressed at 1300 °C and their increase in comparison with specimens processed at 1100 °C is the compromise between the slightly higher relative density, the higher amount of interstitials dissolved throughout the material (especially oxygen) and the grain growth induced by the higher processing temperature. Taking into account the combined effect of all these factors, it can be noticed that, generally, the Ti32-BE samples reach higher strength with respect to Ti32-MA, with the exception of the specimens hot-pressed at 1300 °C where the final mean values are similar.

Finally, the $\sigma_{0.2}$ values obtained for the hot-pressed Ti–3Al–2.5V samples are, normally, higher with respect to the value specified for wrought Ti–6Al–4V or wrought Ti–6Al–7Nb medical devices, whose values range between 900 MPa and 1000 MPa [23].

The maximum bending strength and flexural strain obtained during the three-point bending test of the as-sintered and ground hot-pressed Ti–3Al–2.5V samples are reported in Table 2.

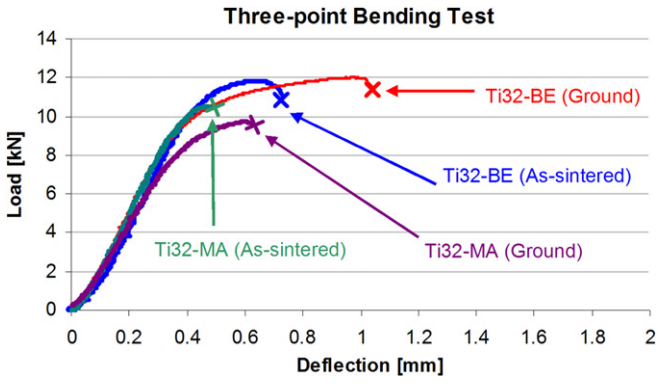

Fig. 11. Representative examples of load–deflection curves for vacuum hot-pressed samples.

Table 2
Maximum bending strength and flexural strain of vacuum hot-pressed samples.

Material		Ti32-BE		Ti32-MA	
		As-sintered	Ground	As-sintered	Ground
Maximum bending strength [MPa]	900 °C	1430 ± 21	1538 ± 7	1264 ± 51	1318 ± 22
	1100 °C	1547 ± 5	1883 ± 77	1345 ± 21	1550 ± 10
	1300 °C	1054 ± 14	1544 ± 120	1005 ± 11	1535 ± 162
Flexural strain [%]	900 °C	2.67 ± 0.21	2.78 ± 0.07	3.65 ± 0.19	2.71 ± 0.07
	1100 °C	3.83 ± 0.10	4.91 ± 1.06	2.68 ± 0.35	3.44 ± 0.62
	1300 °C	2.15 ± 0.09	2.70 ± 0.78	1.99 ± 0.45	2.53 ± 0.45

When comparing the maximum bending strength (Table 2) with the yield strength (Fig. 12), it can be noticed that in some cases, especially for the samples processed at 1300 °C, these two strength values coincide because the alloys behave as brittle materials. In the other cases, the maximum bending strength tends to be higher than the yield strength. The difference is more pronounced for the samples hot-pressed at 1100 °C. Moreover, it can also be seen that, independent of the removal of the surfaces, the maximum bending strength increases when raising the processing temperature from 900 °C to 1100 °C. However, a further increase of the temperature leads to a decrease in strength most likely due to consequent grain growth and the presence of the brittle reacted layer. Once again, the removal of the interaction surface layer is beneficial in order to increase the strength of the material and, as it was for the yield strength, Ti32-BE reaches higher strength in comparison with Ti32-MA.

Concerning the flexural strain values of hot-pressed Ti–3Al–2.5V samples shown in Table 2, it can be seen that this property follows the same trend as the maximum bending strength, increasing from 900 °C to 1100 °C and then decreasing for higher processing temperatures. The behaviour can be well explained using the chemical analysis results because the content of the elements with the strongest effect on ductility, oxygen and nitrogen [24,25], does not increase significantly at 1100 °C but then does for the processing temperature of 1300 °C. Finally, the removal of the surfaces of the specimens leads also to an improvement in ductility of Ti–3Al–2.5V alloy.

4. Conclusions

1. This study demonstrates that irregular shaped Ti–3Al–2.5V powders produced by the blending elemental or the master alloy addition approaches are suitable for obtaining almost fully dense materials when processed by vacuum hot-pressing. The relative density values obtained are, therefore, normally higher in comparison with those of uniaxially pressed and sintered components.
2. From the microstructural analysis, the typical laminar microstructure of the wrought Ti–3Al–2.5V can be obtained. Nevertheless, to guarantee the complete diffusion and homogenisation of the alloying elements the powders must be processed at 1300 °C.
3. The employment of an HDH prealloyed Ti–6Al–4V powder as master alloy for the production of the Ti–3Al–2.5V alloy leads to enhanced mechanical properties in comparison with those achieved with the utilisation of an Al:V master alloy.
4. Independently of the alloying elements addition approach employed, titanium reacts with the BN coating normally used to prevent the direct contact between titanium and graphite tools. The interaction between titanium and BN leads to the formation of a reacted layer composed by titanium nitrides and borides, which makes the material more brittle.
5. Hot-pressing can be employed as an alternative way to produce near-net-shape, chemically homogeneous and fine-grained Ti–3Al–2.5V components starting from HDH powders. The employment of the blending elemental approach should also lead to a reduction in the fabrication costs of titanium products.

Acknowledgements

The authors are thankful for the financial support from Comunidad de Madrid through the ESTRUMAT (S-2009/MAT-1585) project and from the Spanish Ministry of Education through the R&D MAT2009-14448-C02-02 and MAT2009-14547-C02-02 Projects.

References

[1] G. Lütjering, J.C. Williams, Titanium: Engineering Materials and Processes, first ed., Springer, Manchester, UK, 2003.
[2] M.J. Donachie, Titanium. A Technical Guide, second ed., ASM International, Ohio, USA, 2000.
[3] M. Niinomi, Mechanical properties of biomedical titanium alloys, Materials Science and Engineering A 243 (1998) 231–236.
[4] R. Boyer, G. Welsch, E.W. Collings, Materials Properties Handbook: Titanium Alloys, A. International, Ohio, USA, 1998.
[5] R.M. German, Powder Metallurgy of Iron and Steel, John Wiley & Sons, Inc, 1998.
[6] W. Schatt, K.-P. Wieters, Powder Metallurgy. Processing and Materials, EPMA – European Powder Metallurgy Association, Shrewsbury, UK, 1997.
[7] C.G. Goetzel, V.S. de Marchi, Electrically activated pressure sintering (spark sintering) of titanium powders, Powder Metallurgy International 3 (1971) 80–87.
[8] W.H. Kao, D. Eylon, C.F. Yolton, F.H. Froes, Effect of temporary alloying by hydrogen (HYDRO-VAC) on the vacuum hot pressing and microstructure of titanium alloy powder compacts, Progress in Powder Metallurgy 37 (1982) 289–301.
[9] C.G. Goetzel, V.S. de Marchi, Electrically activated pressure sintering (spark sintering) of titanium–aluminium–vanadium alloy powders, Modern Developments in Powder Metallurgy 4 (1971) 127–150.
[10] R.K. Malik, Hot pressing of titanium aerospace components, The International Journal of Powder Metallurgy & Powder Technology 10 (1974) 115–129.
[11] L. Bolzoni, P.G. Esteban, E.M. Ruiz-Navas, E. Gordo, Influence of powder characteristics on sintering behaviour and properties of PM Ti alloys produced from prealloyed powder and master alloy, Powder Metallurgy 54 (2011) 543–550.
[12] S. Abkowitz, D. Rowell, Superior fatigue properties for blended elemental P/M Ti–6Al–4V, Journal of Metals (1986) 36–39.
[13] K.T. Kim, H.C. Yang, Densification behavior of titanium alloy powder during hot pressing, Materials Science and Engineering A 313 (2001) 46–52.
[14] A. Bose, W.B. Eisen, Hot Consolidation of Powders & Particulates, Metal Powder Industries Federation, Princeton, USA, 2003.
[15] R.I. Jaffee, The physical metallurgy of titanium alloys, Progress in Metal Physics 7 (1958) 65–163.
[16] H. Sibum, V. Güther, O. Roidl, F. Habashi, H.-U. Wolf, Titanium, Titanium Alloys, and Titanium Compounds, 2002.
[17] J.L. Murray, Phase Diagrams of Binary Titanium Alloys, first ed., ASM International, 1987.
[18] V. Tomashik, Boron–nitrogen–titanium. Available at: http://www.springermaterials.com/pdfs/10.1007/978-3-642-02700-0_7.pdf, 2010.
[19] A.L. Borisova, Y.S. Borisov, L.K. Shvedova, I.S. Martsenyuk, Reactions in powder Ti–BN composites, Powder Metallurgy and Metal Ceramics 4 (1984) 18–22.
[20] E. Benko, Calculations of Chemical Equilibria in BN–Ti System, Powder Metallurgy World Congress, Paris, 1994, pp. 14–72.
[21] E. Faran, I. Gotman, E.Y. Gutmanas, Experimental study of the reaction zone at boron nitride ceramic–Ti metal interface, Materials Science and Engineering A 288 (2000) 66–74.
[22] L. Bolzoni, E.M. Ruiz-Navas, E. Neubauer, E. Gordo, Inductive hot-pressing of titanium and titanium alloy powders, Materials Chemistry and Physics 131 (2012) 672–679.
[23] ASM International, Materials and Coatings for Medical Devices: Cardiovascular, ASM International, Ohio, USA, 2009.
[24] R.I. Jaffee, I.E. Campbell, The effect of oxygen, nitrogen and hydrogen on iodide refined titanium, Transactions of the American Institute of Mining and Metallurgical Engineers 185 (1949) 646–654.
[25] R.I. Jaffee, H.R. Ogden, D.J. Maykuth, Alloys of titanium with carbon, oxygen and nitrogen, Transactions of the American Institute of Mining and Metallurgical Engineers 188 (1950) 1261–1266.